SUPPLEMENTAL MATERIAL

Manuscript ID : CIRCULATIONAHA/2010/014050

Involvement of Endoplasmic Stress Protein CHOP in Arteriosclerosis Acceleration with Augmented Biological Stress Responses

First Author: Junhong Gao

Table 1

Probe	Primer 1	Primer 2
MCP-1	5'ACTGAAGCCAGCTCTCTCTTCCTC3'	5'TTCCTTCTTGGGGTCAGCACAGAC3'
IL-6	5'CAATGCTCTCCTAACAGATAAG-3'	5'AGGCATAACGCACTAGGT3'
IL-1β	5'CAAGCAATACCCAAAGAAGA-3'	5'-GAAACAGTCCAGCCCATAC-3'
CATALASE	5'-AGGTGTTGAACGAGGAGGA-3'	5'-CTCAGCGTTGTACTTGTCCA-3'
GST	5'-TGCCAAGATCAAGGAACAAA-3'	5'-CCACATGGTAGAGGAGTTCAA-3'
SOD	5'-GGTCGCTTACAGATTGCT-3'	5'-CTCCCAGTTGATTACATTCC-3'
CRP	5'-CAGCTTCTCTCGGACTTTTG-3'	5'-AGGTGTTCAGTGGCTTCTTTG-3'
GAPDH	5'- ACCACAGTCCATGCCATCAC -3'	5'- TCCACCACCCTGTTGCTGTA -3'
h-GAPDH	5'GGC TGC TTT TAA CTC TGG T 3'	5'AGA TGG TGA TGG GAT TTC 3
h-CHOP	5' ACC CTG CTT CTC TGG CTT 3'	5' GGG GAA TGA CCA CTC TGT 3'
h-PDGFbeta	5' CCA GGT GAG AAA GAT CGA GA 3'	5' AAT GGT CAC CCG AGT TTG 3'
h-PDGF-RB	5' CAA TGA GGG TGA CAA CGA CT 3'	5' ATG GTT GAG GAG GTG TTG ACT 3'
h-PDGF-alpha	5' CAG GAC GGT CAT TTA CGA 3'	5' TTG GCT TCT TCC TGA CGT AT 3'
h-TGF-beta1	5' CAA TTC CTG GCG ATA CCT 3'	5' TGT GTT ATC CCT GCT GTC A 3'
Egr1	5' CGA GCG AAC AAC CCT ATG 3',	5' AGC GGC CAG TAT AGG TGA 3'
SDF-1a	5' GGT TCT TCG AGA GCC ACA T 3'	5' TTC GGG TCA ATG CAC ACT 3'
ERO1	5' TGG AGC CGT GGA TGA GTC T 3',	5' CAG CAT CGG GGG ACT GTA T 3'
F4/80	5' CAT CAT GGC ATA CCT GTT CAC 3',	5' GAA TGG GAG CTA AGG TCA GTC 3'
KLF5	5' AAA CTG GCG ATT CAC AAC 3',	5' CAG GTG AGC TTT TAA GTG AG 3'
TGF-beta	5' GTG GAG CAA CAT GTG GAA CT 3',	5' AAA GCC CTG TAT TCC GTC T 3'
PDGF-a	5' GGC TCG AAG TCA GAT CCA C 3',	5' CTT CTC GGG CAC ATG GTT 3'
Lox-1	5' CAA GCA ATT TCC CAT ACC AC 3',	5' TCC GTC TTG AAG GTA TGC AC 3'
PDGF-beta	5' TGA AAT GCT GAG CGA CCA 3',	5' GCT CGG GTC ATG TTC AAG T 3'
PDGF-RB	5' AGC CTG ACG TTG CTG ATG 3',	5' CTT GCT GTG GCT CTT CTT G 3'
SRA1	5' AGG GAG ACA GAG GGC TTA CT 3',	5' GCC TAC ACT CCC CTT CTC T 3'
VCAM-1	5' GGA AGC TGG AAC GAA GTA 3',	5' CAA TCT CCA GCC TGT AAA CT 3'
ICAM-1	5' GCT GCT ACC TGC ACT TTG 3',	5' GGA TGG ATG GAT ACC TGA 3'
E-selectin	5' CAT CGT CCT CAT TGC TCT A 3',	5' AGA CGT TGT AAG AAG GCA C 3'

Figure I

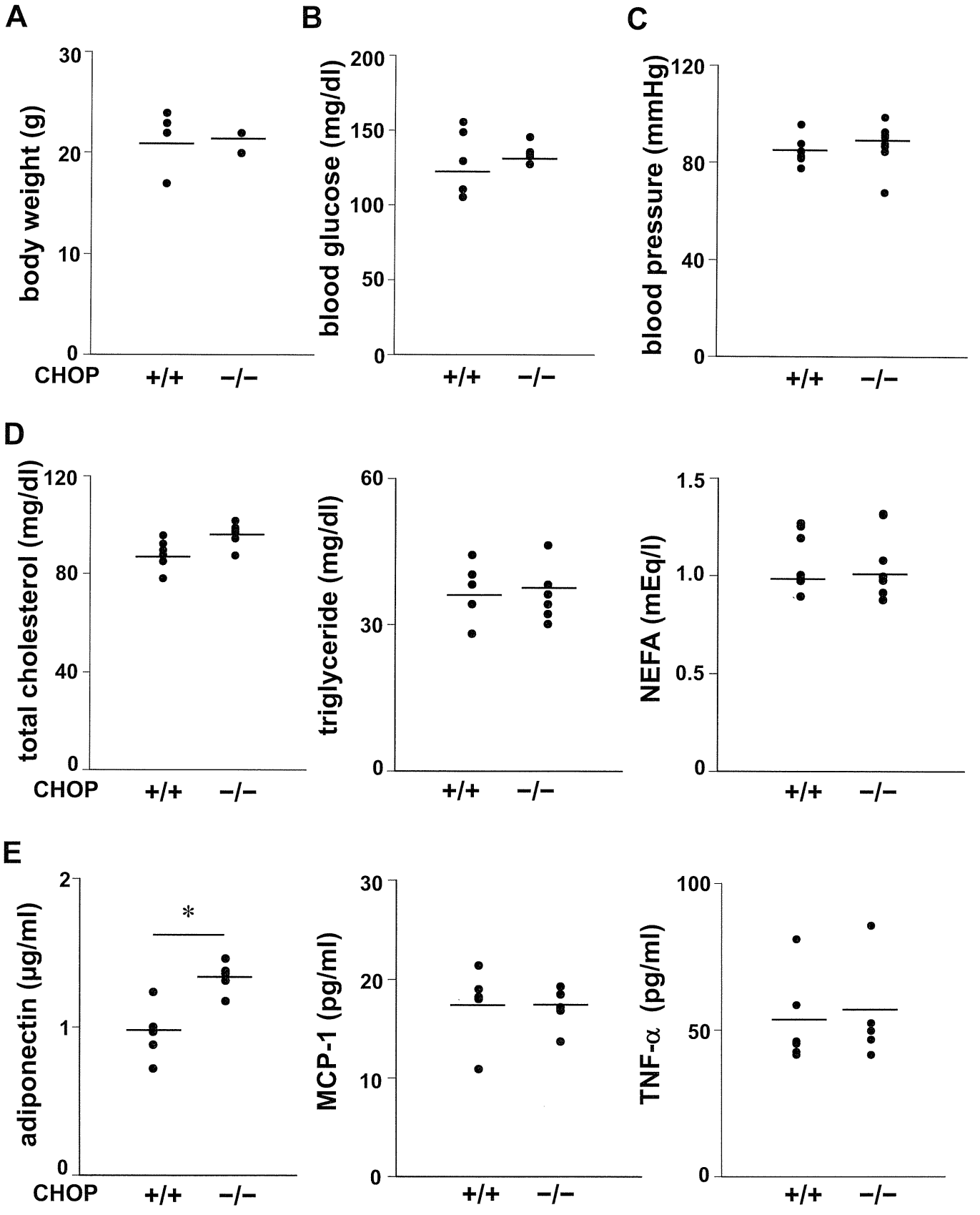

Figure II

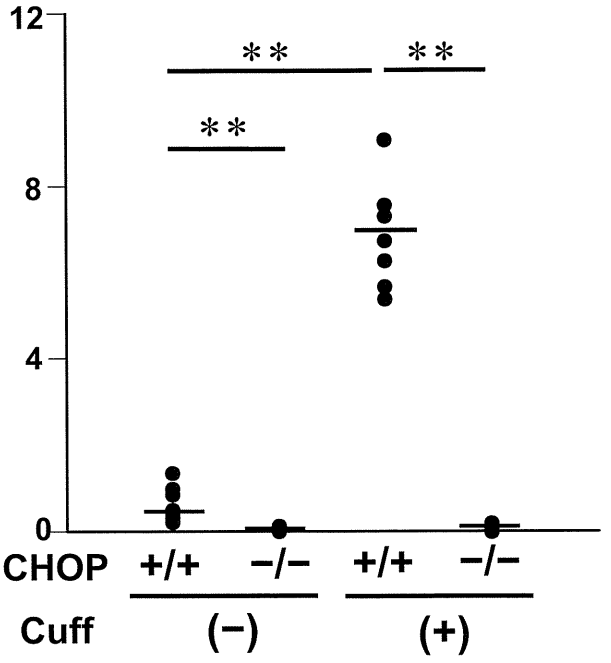

Figure III

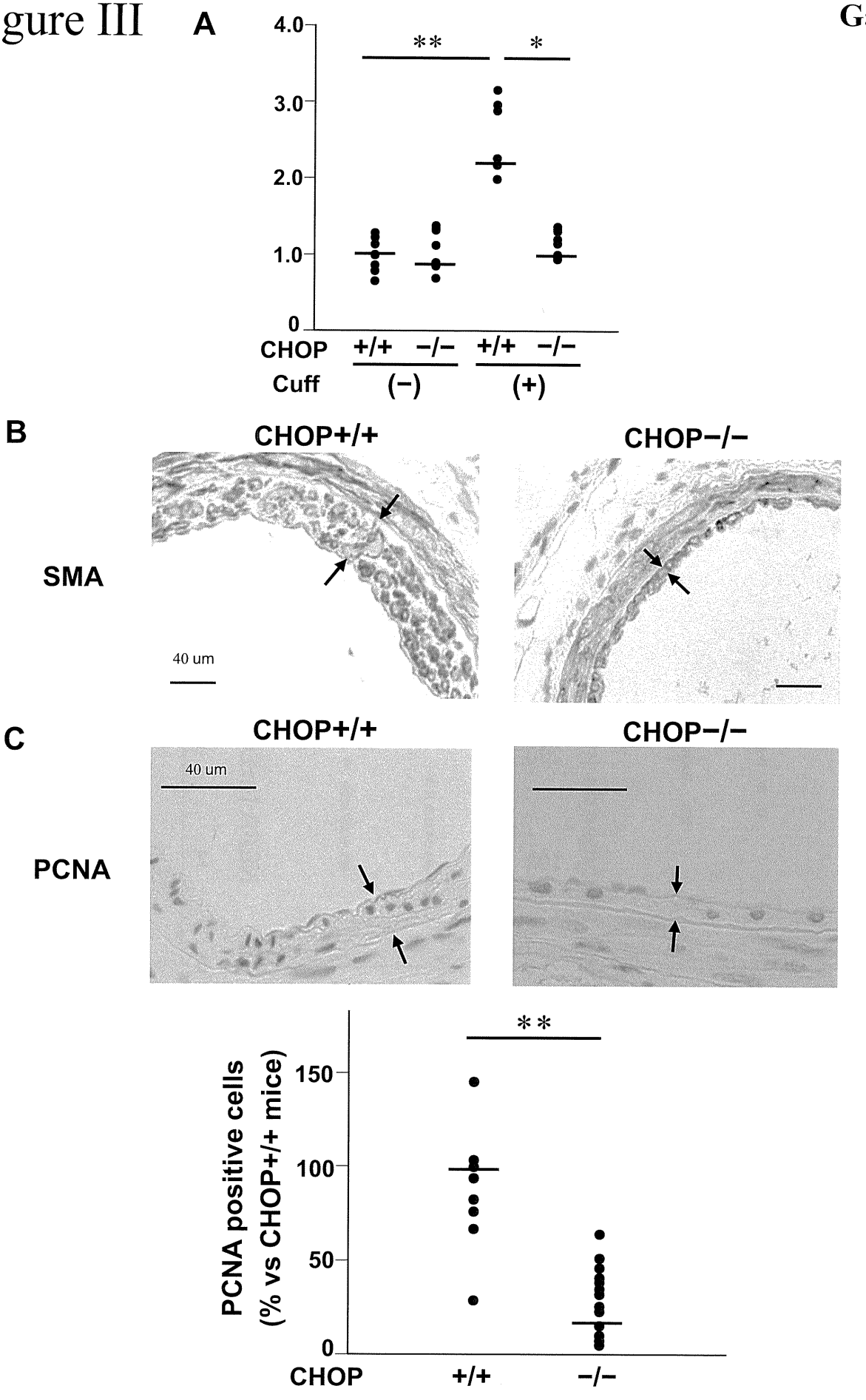

Figure IV

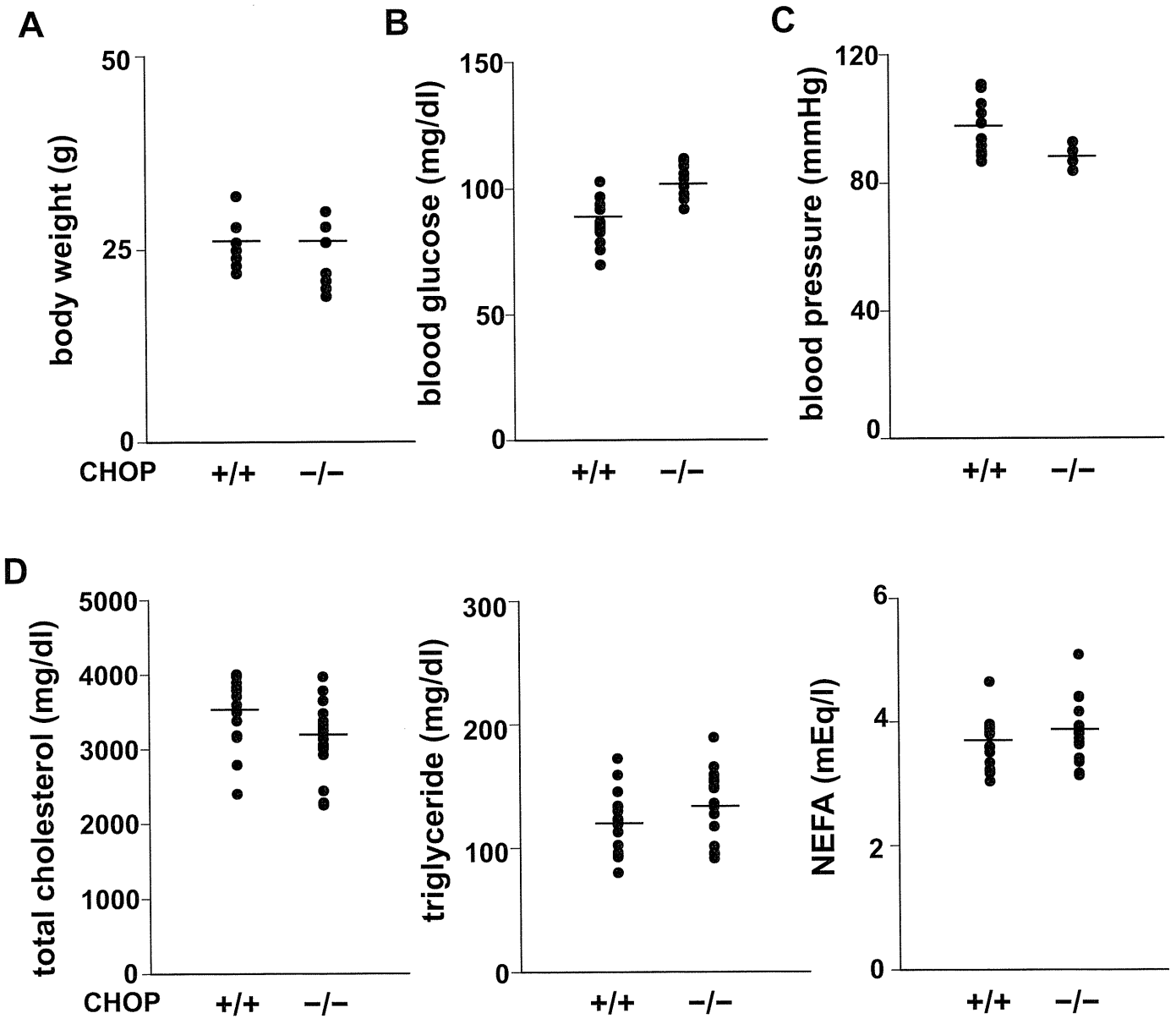

Figure V

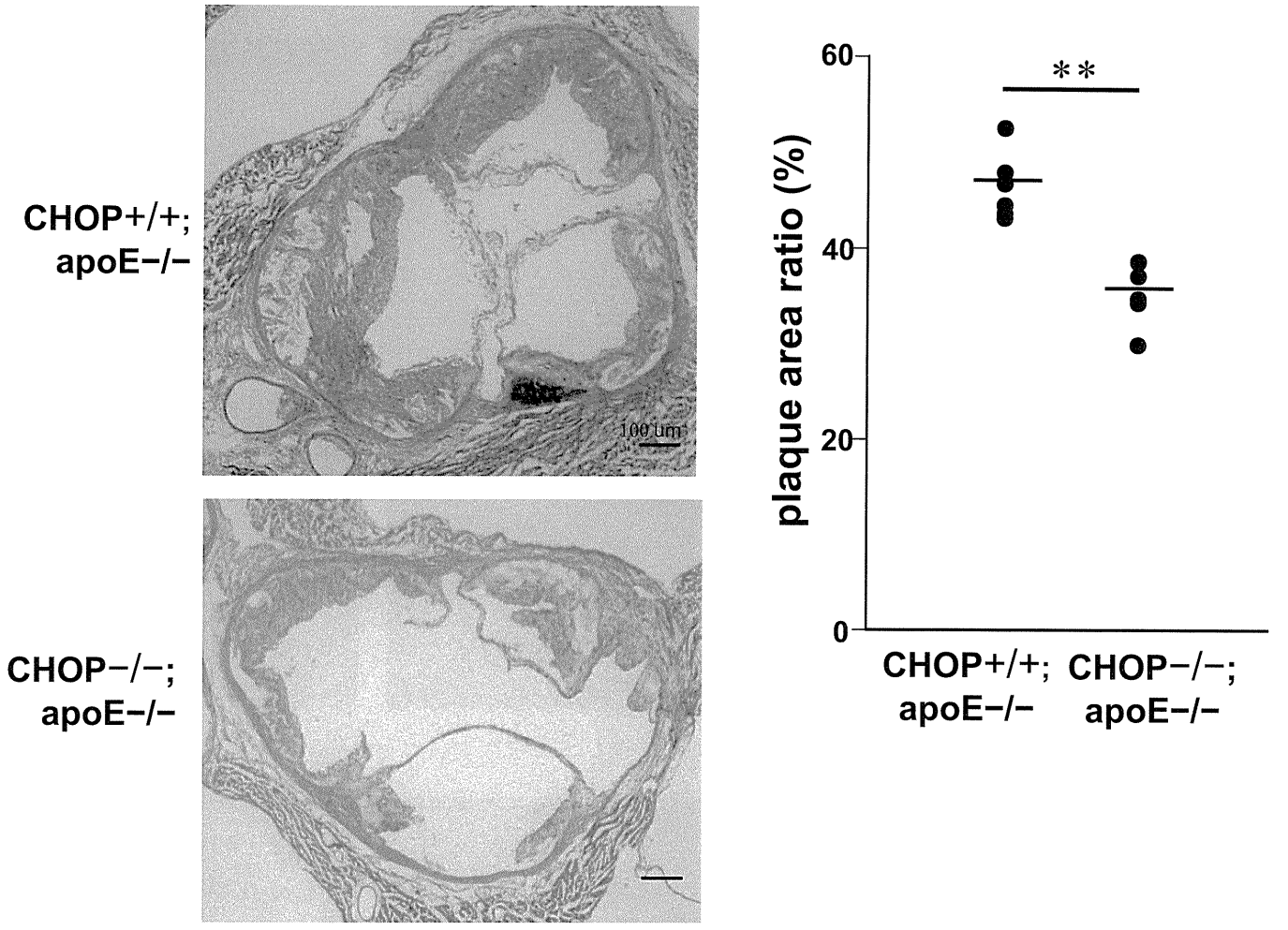

Figure VI-A

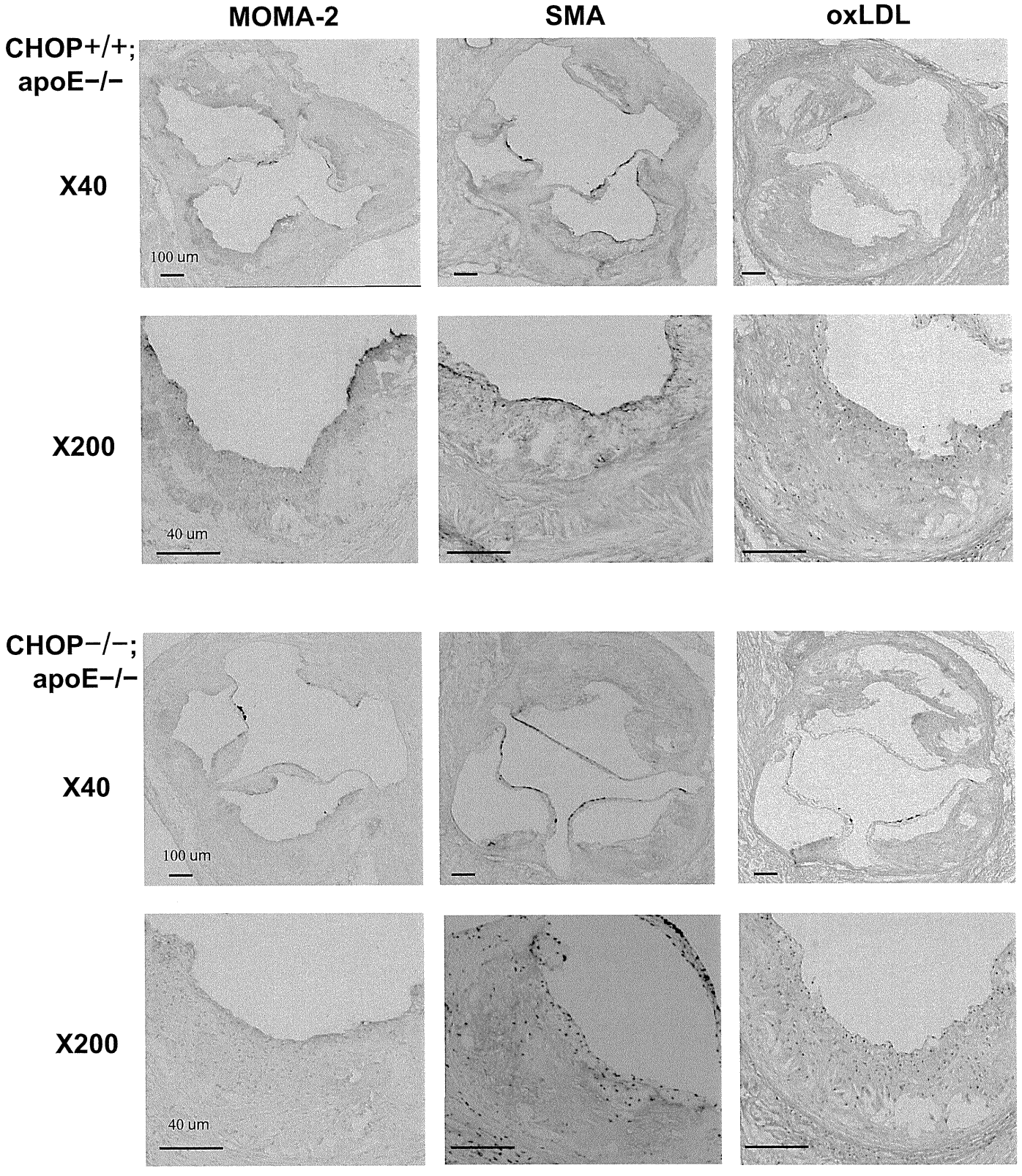

Figure VI-B

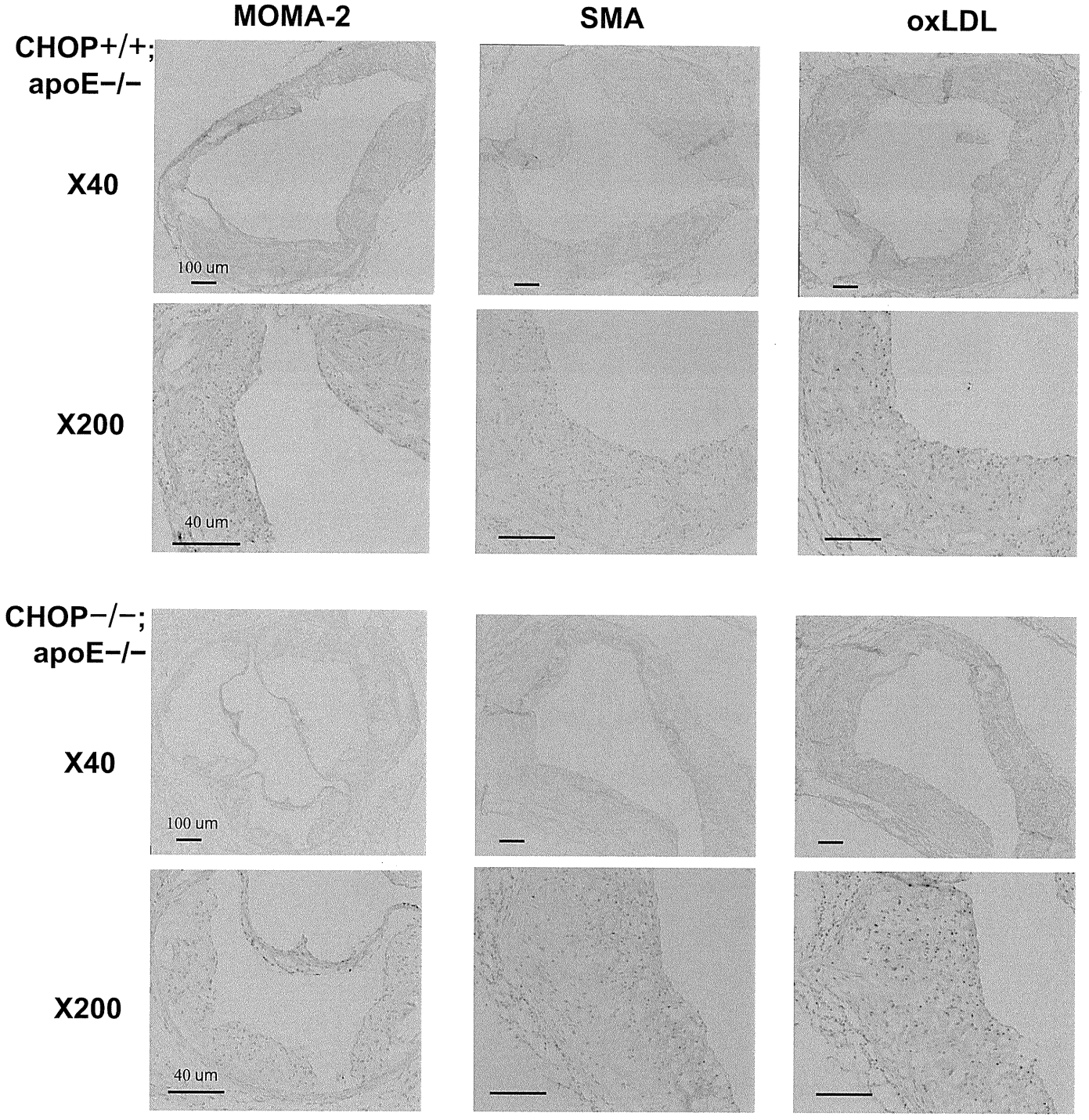

Figure VII

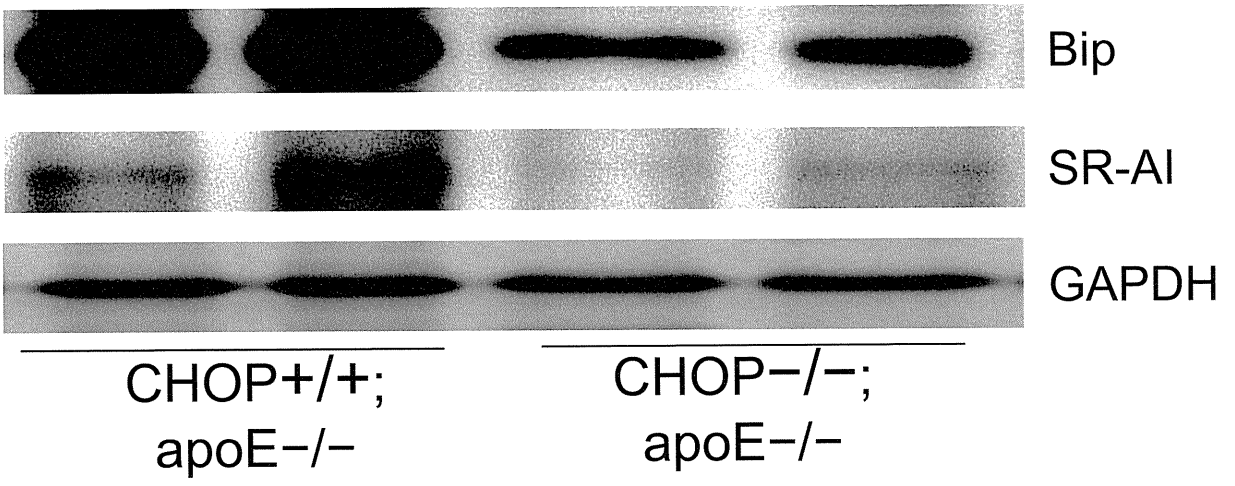

Figure VIII

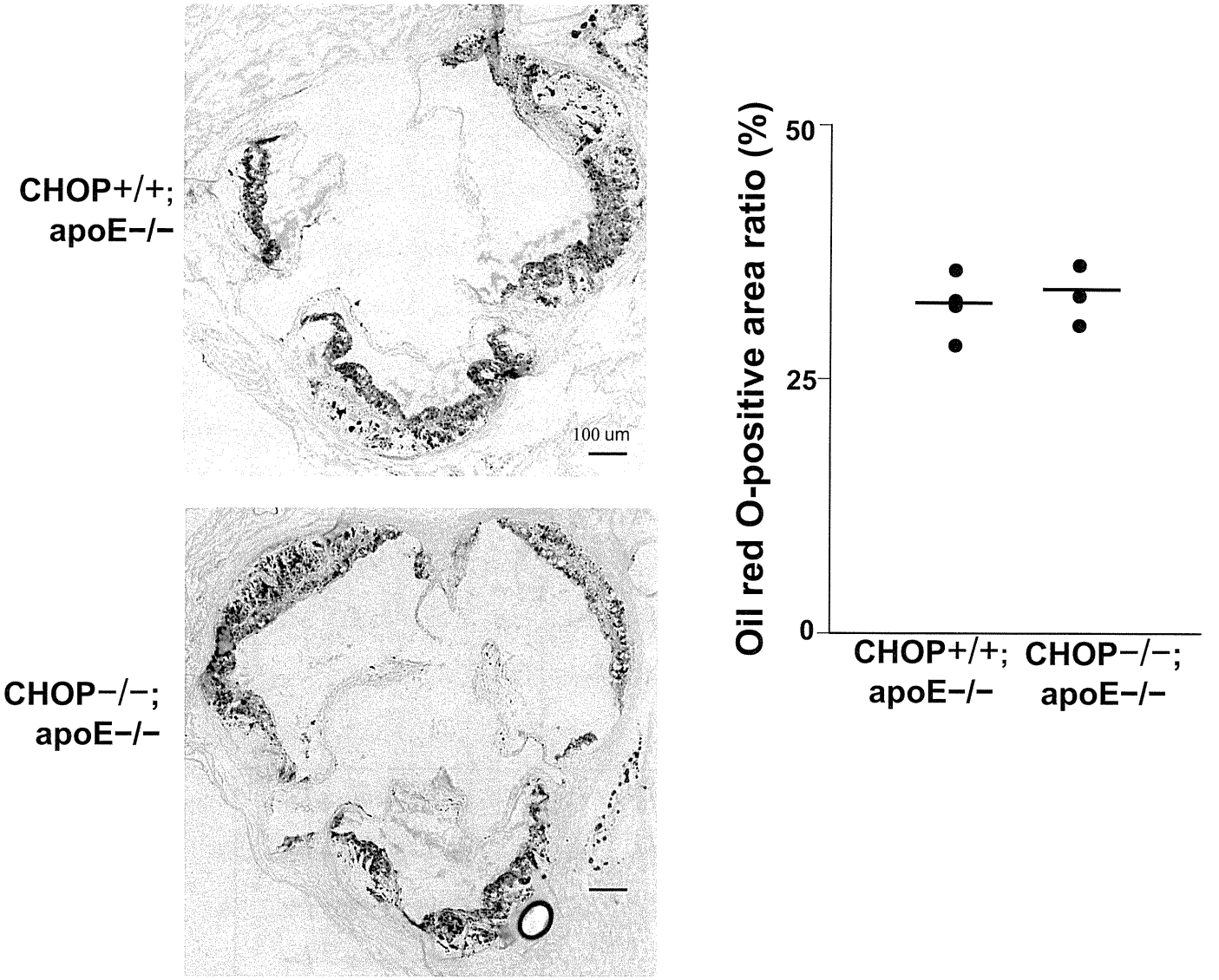

Figure IX

A

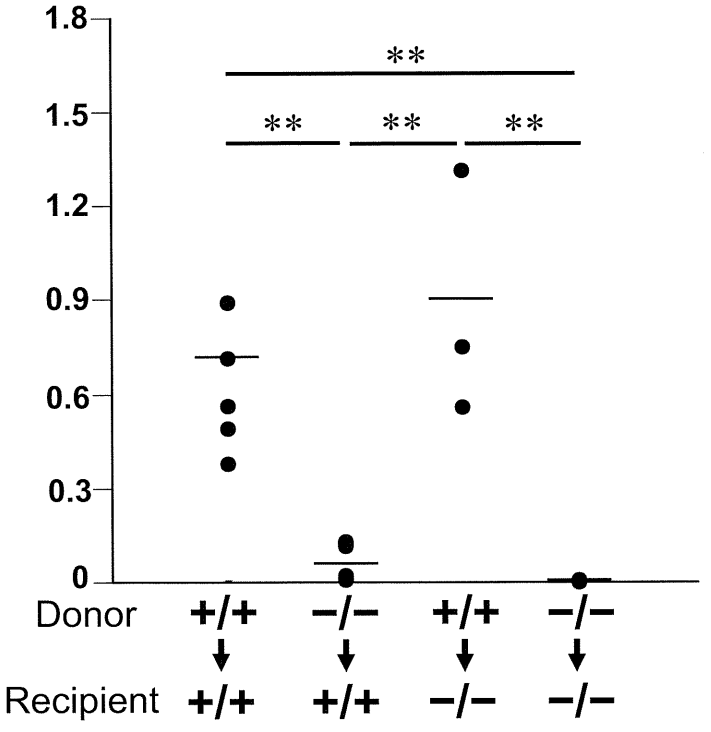

B

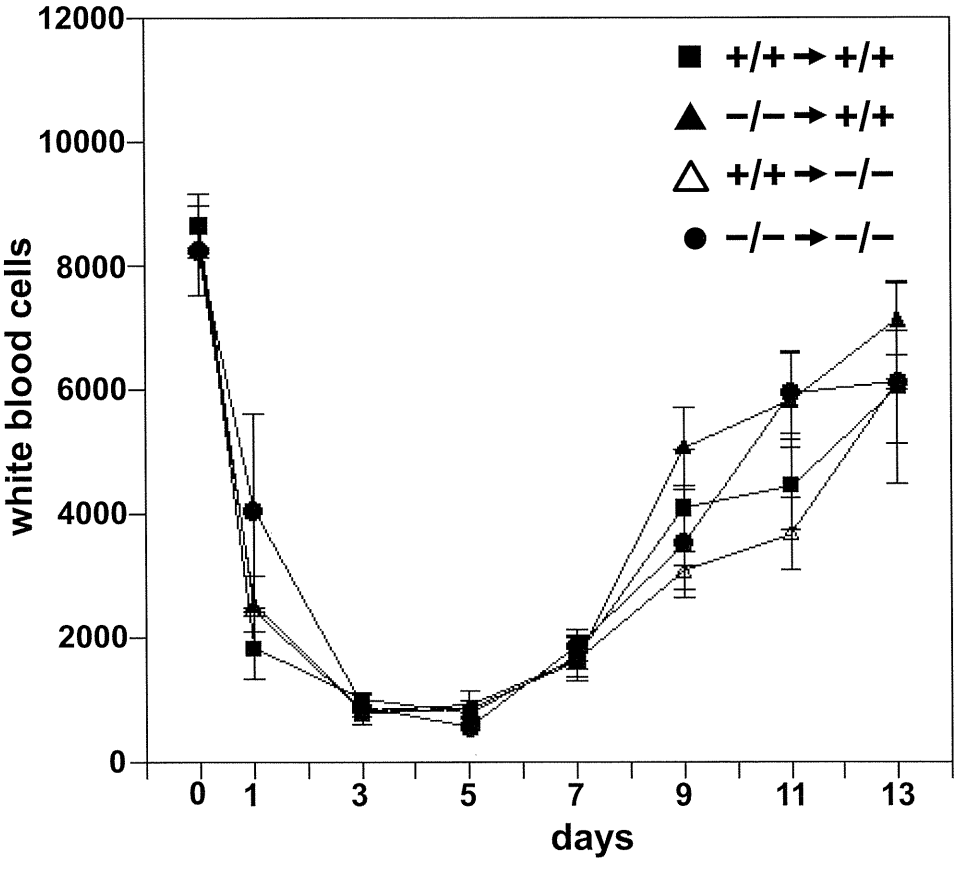

Figure X

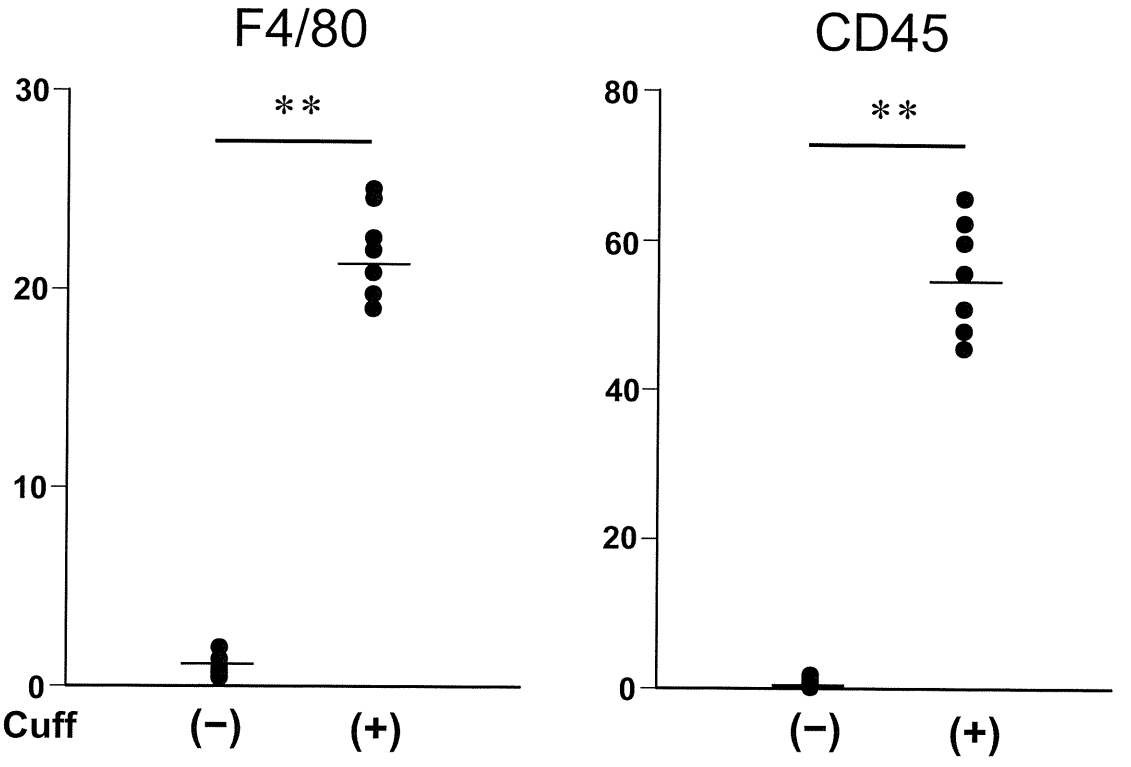

Figure XI

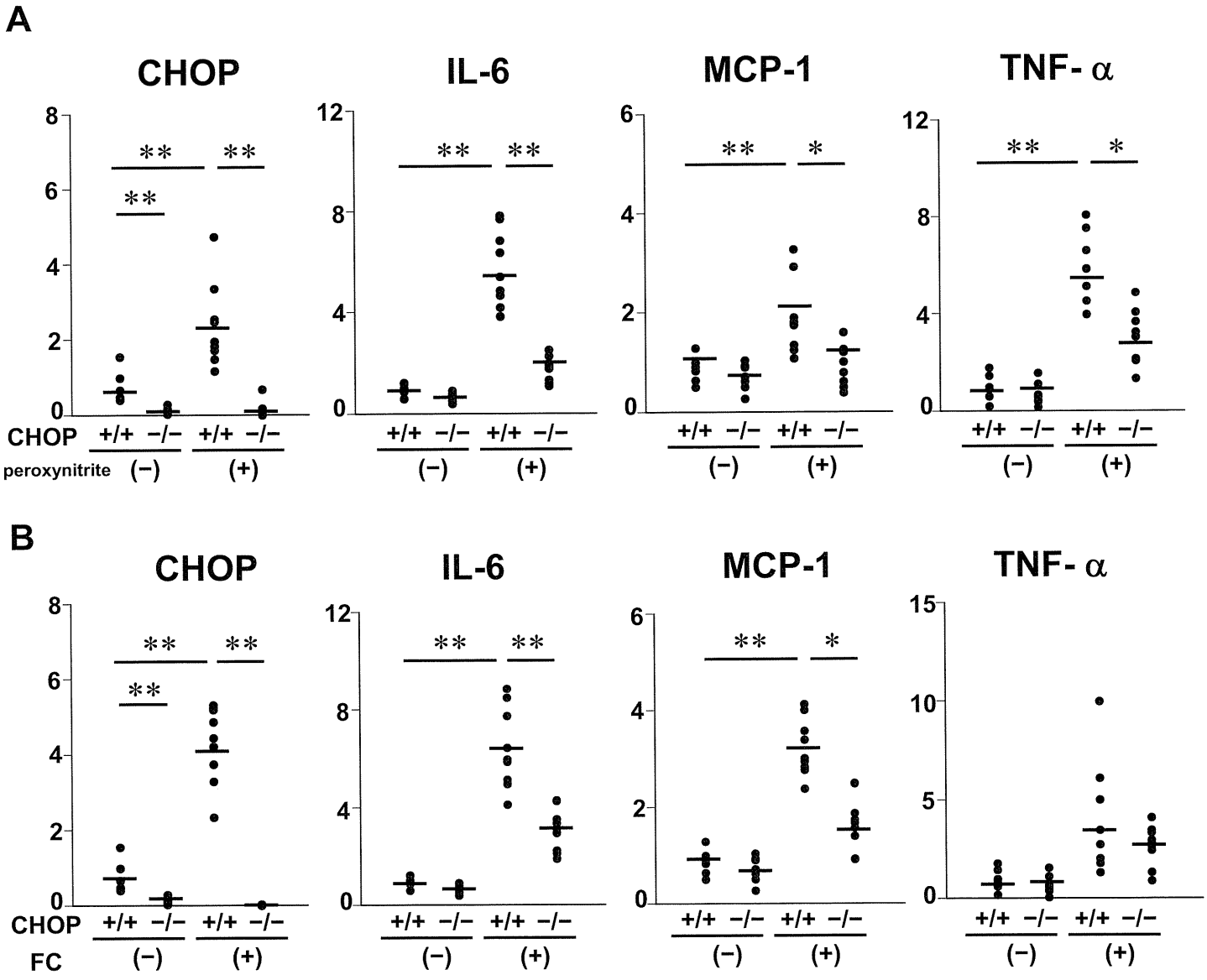

Supplemental Material

Supplemental Figure Legends

Figure I CHOP deficiency caused no gross phenotypic differences

CHOP+/+ and CHOP-/- (n=5 per group) mice were fed normal chow and subjected to measurement of body weight (A), blood glucose (B), blood pressure (C), plasma levels of lipid parameters (D) such as total cholesterol (left), triglyceride (middle) and non-esterified fatty acids (NEFA) (right), and plasma levels of adipokines (E), such as adiponectin (left), MCP-1 (middle) and TNF-α (right), at 11 weeks of age. Data are presented as means ± SE.*$P < 0.05$ by the unpaired t test.

Figure II Arterial CHOP expression was up-regulated by cuff injury

Arterial expression of CHOP in cuff-injured and uninjured arteries of CHOP+/+ and CHOP-/- (n=7 per group) mice 7 days after cuff placement were quantified by RT-PCR. Data are presented as means ± SE. **$P < 0.01$ by one-way ANOVA.

Figure III Cuff injury-induced neointimal SMC proliferation was suppressed in CHOP deficient mice

Expressions of α-smooth-muscle isoform of actin (SMA) in cuff-injured and uninjured arteries 3 weeks after cuff placement in CHOP+/+ and CHOP-/- (n=7 per group) mice were quantified by RT-PCR adjusted with GAPDH (A). Immunological stainings against SMA (B) and PCNA (C; upper panel) were prepared from cuff injured femoral arteries 3 weeks after placement in CHOP+/+ (left) and CHOP-/- (right) mice. The relative amounts of PCNA positive cells in neointimal lesions (n=14) were presented as the ratio to CHOP +/+ mice (n=9) (C; lower panel). *$P < 0.05$, **$P < 0.01$ by the

unpaired *t* test or one-way ANOVA.

Figure IV CHOP deficiency caused no gross phenotypic differences in apoE-/- mice

CHOP+/+;apoE-/- (*n*=18) and CHOP-/-;apoE-/- (*n*=13) mice were fed 1.25% high cholesterol chow starting at 8 weeks of age and subjected to measurement of body weight (A), blood glucose (B), blood pressure (C), plasma levels of lipid parameters (D) such as total cholesterol (left), triglyceride (middle), and non-esterified fatty acids (NEFA) (right). Data are presented as means ± SE.

Figure V Aortic root cross-sections from 20-week-old CHOP+/+;apoE-/- and CHOP-/-;apoE-/- mice

Aortic root cross-sections were prepared from 20-week-old CHOP+/+;apoE-/- (*n*=5) and CHOP-/-;apoE-/- (*n*=5) mice and stained with hematoxylin and eosin. Representative histological findings are shown in the left panels. Atherosclerosis was evaluated as plaque areas, which were expressed as percentages of the total lumen areas in CHOP+/+;apoE-/- (*n*=5) and CHOP-/-;apoE-/- (*n*=5) mice. Data are presented as means ± SE. $^{**}P < 0.01$ by the unpaired *t* test.

Figure VI Immunohistological findings of aortic plaque lesions from 20-week-old CHOP+/+;apoE-/- and CHOP-/-;apoE-/- mice

Aortic sections from 20-week-old CHOP+/+;apoE-/- (upper panels) and CHOP-/-;apoE-/- (lower panels) mice fed 1.25% high cholesterol chow were immunostained with antibodies against MOMA-2 (left), SMA (middle) or oxidized LDL (right) (A). A series of immunological staining with control antibodies, i.e. rat IgG2b as

a control for MOMA-2 (left), mouse IgG2a as a control for SMA (middle), rabbit immunoglobulin as a control for oxidized LDL (right), were performed in the corresponding aortic samples (B). Magnifications of upper and lower panels are x40 and x200, respectively. Representative immunostaining findings from all samples (n=7 per group) are shown.

Figure VII Protein expressions of Bip and SR-AI in the aorta

Tissue protein extracts of whole aorta samples from 24-week-old CHOP+/+;apoE-/-, CHOP-/-;apoE-/- mice were subjected to immunoblotting with antibodies to Bip (upper panels), SR-AI (middle panels) and GAPDH as a loading control (lower panel).

Figure VIII Aortic root cross-sections from 14-week-old CHOP+/+;apoE-/- and CHOP-/-;apoE-/- mice

Aortic root cross-sections were prepared from 14-week-old CHOP+/+;apoE-/- and CHOP-/-;apoE-/- mice and stained with oil red O. Representative histological findings are shown in the left panels. Atherosclerosis was evaluated as oil red O-stained areas, which were expressed as percentages of the total lumen areas in CHOP+/+;apoE-/- (n=3) and CHOP-/-;apoE-/- (n=3) mice. Data are presented as means ± SE.

Figure IX Reconstitution of BM cells 2weeks after BMT

Bone marrow cell expressions of CHOP 2 weeks after BMT were quantified by RT-PCR in CHOP+/+ to CHOP+/+ (n=5), CHOP-/- to CHOP+/+ (n=5), CHOP +/+ to CHOP-/- (n=3) and CHOP-/- to CHOP-/- (n=3) BMT mice (A). Time course of peripheral WBC counts from the day before BMT to 13 days after BMT (B). Data are presented as means

± SE. $^{**}P < 0.01$ by one-way ANOVA.

Figure X Macrophage and hematopoietic cell markers before and after cuff placement

Arterial expressions of F4/80 and Ptprc (CD45) before (2 weeks after BMT) (n=6), and 3 weeks after (n=8) cuff placement were quantified by RT-PCR in CHOP+/+ to CHOP+/+ BMT mice. Data are presented as means ± SE. $^{**}P < 0.01$ by the unpaired t test.

Figure XI

CHOP deficiency suppressed peroxynitrite- and free cholesterol-induced inflammatory responses of macrophages.

mRNA expressions of CHOP and inflammatory cytokines in peritoneal macrophages from CHOP+/+ (n=9) and CHOP-/- (n=9) mice in response to peroxynitrite (A) and free cholesterol (B) treatments, were evaluated by RT-PCR. Peritoneal macrophages from CHOP+/+ (n=5) and CHOP-/- (n=6) mice without these ER stress-inducing agents were also subjected to analyses of mRNA expressions. $^{*}P < 0.05$, $^{**}P < 0.01$ by the one-way ANOVA.

European Heart Journal Advance Access published August 8, 2011

European Heart Journal
doi:10.1093/eurheartj/ehr265

BASIC SCIENCE

Hepatic peroxisome proliferator-activated receptor-γ–fat-specific protein 27 pathway contributes to obesity-related hypertension via afferent vagal signals

Kenji Uno[1,2], Tetsuya Yamada[1], Yasushi Ishigaki[2], Junta Imai[2], Yutaka Hasegawa[2], Junhong Gao[1], Keizo Kaneko[2], Kimihiko Matsusue[3], Tomomi Yamazaki[4], Yoshitomo Oka[2], and Hideki Katagiri[1]*

[1]Department of Metabolic Diseases, Center for Metabolic Diseases, Tohoku University Graduate School of Medicine, 2-1 Seiryo-machi, Aoba-ku, Sendai 980-8575, Japan; [2]Division of Molecular Metabolism and Diabetes, Tohoku University Graduate School of Medicine, Sendai 980-8575, Japan; [3]Faculty of Pharmaceutical Science, Fukuoka University, Fukuoka 814-0180, Japan; and [4]Nutritional Science Program, National Institute of Health and Nutrition, Tokyo 162-8636, Japan

Received 26 October 2010; revised 17 June 2011; accepted 7 July 2011

Aims Obesity is commonly associated with hypertension. Increased sympathetic tonus in obese subjects contributes to the underlying mechanism. However, the precise mechanisms whereby obesity induces this sympathetic activation remain unclear. Hepatic peroxisome proliferator-activated receptor (PPAR)-γ2 expression, which is reportedly upregulated during obesity development, affects sympathetic activation via hepatic vagal afferents. Herein, we report involvement of this neuronal relay in obesity-related hypertension.

Methods and results Peroxisome proliferator-activated receptor-γ and a direct PPARγ target, fat-specific protein 27 (Fsp27), were adenovirally overexpressed or knocked down in the liver, in combination with surgical dissection or pharmacological deafferentation of the hepatic vagus. Adenoviral PPARγ2 expression in the liver raised blood pressure (BP) in wild-type but not in β1/β2/β3 adrenergic receptor-deficient mice. In addition, knockdown of endogenous PPARγ in the liver lowered BP in murine obesity models. Either surgical dissection or pharmacological deafferentation of the hepatic vagus markedly blunted BP elevation in mice with diet-induced and genetically-induced obesity. In contrast, BP was not elevated in other models of hepatic steatosis, DGAT1 and DGAT2 overexpressions, in which PPARγ is not upregulated in the liver. Thus, hepatic PPARγ upregulation associated with obesity is involved in BP elevation during obesity development. Furthermore, hepatic expression of Fsp27 raised BP and the effect was blocked by hepatic vagotomy. Hepatic Fsp27 is actually upregulated in murine obesity models and its knockdown reversed BP elevation.

Conclusion The hepatic PPARγ–Fsp27 pathway plays important roles in the development of obesity-related hypertension via afferent vagal signals from the liver.

Keywords Obesity • Hypertension • Neuronal signals • PPARγ • Fsp27

Introduction

The worldwide prevalence of obesity is increasing at an alarming rate, with major adverse consequences including atherosclerotic morbidity, i.e. coronary heart disease and central vascular disease.[1] In particular, visceral obesity is prone to be associated with hypertension, glucose intolerance and dyslipidaemia, collectively termed the metabolic syndrome, the combination of which increases the risk for cardiovascular morbidities. Numerous mechanisms have been proposed to underlie obesity-related

* Corresponding author. Tel: +81 22 717 8228, Fax: +81 22 717 8228, Email: katagiri@med.tohoku.ac.jp

hypertension. These include increased sodium reabsorption, activation of the renin–angiotensin–aldosterone system, oxidative and inflammatory stress, endothelial dysfunction and decreased sensitivity to natriuretic peptides.[2,3] Adiposity-induced insulin resistance and the resulting hyperinsulinaemia also reportedly contribute to these mechanisms.[4] In addition, adiposity impairs adipocyte function and alters the adipokine profile, which is also involved in blood pressure (BP) elevation.[5] In particular, there is a strong correlation between plasma leptin concentrations and hypertension in human subjects.[6,7] Thiazolidindione treatment, which promotes adipocyte differentiation, reportedly lowers BP.[8,9] In addition to these humoral mechanisms, it is well known that sympathetic tonus is increased in obese subjects,[10] especially those with visceral adiposity.[11] Such sympathetic activation enhances cardiac output, renal sodium reabsorption, and vasoconstriction as well as potentiating the renin–angiotensin–aldosterone system, leading to the development of hypertension.[12] However, the precise mechanisms whereby obesity induces this sympathetic activation remain unclear.

Obesity is thought to be a disturbed state of energy metabolism homeostasis. To maintain metabolic homeostasis in the whole body, communication among organs/tissues, allowing coordinated metabolic regulation, appears to be essential. In addition to humoral factors, including insulin and adipokines, the autonomic nervous system is now increasingly being recognized as an important component of inter-organ metabolic communication.[1]

In particular, afferent neural signals originating in the liver play important roles in regulating energy[13] and glucose[14] homeostasis. We reported that adenoviral expression of peroxisome proliferator-activated receptor-γ (PPARγ) in the liver enhances both systemic energy expenditure and lipolysis in adipose tissue, via sympathetic activation mediated by the afferent vagus originating in the liver.[13] Although expression of PPARγ, a transcription factor which activates genes involved in lipid storage and production, is very low in the liver when compared with that in adipose tissues,[15] hepatic expression of PPARγ, especially PPARγ2,[16] is upregulated in a number of murine obesity models as well as in obese human subjects.[17] Therefore, this inter-organ communication system via the neuronal relay, consisting of vagal afferents and sympathetic efferents, likely has a role in preventing obesity development by increasing energy expenditure and lipolysis. Herein, we report that this neuronal relay, which may act as a protective mechanism against obesity development, ironically contributes to obesity-related hypertension, a major feature of the metabolic syndrome, via sympathetic activation.

Methods

Due to space requirements, some methodological details have been placed online.

Animals

Animal studies were conducted in accordance with Tohoku University institutional guidelines. Male C57BL/6N, KK, and KK-Ay mice were purchased from Japan Clea (Tokyo, Japan). Male Zucker diabetic fatty (ZDF) and Zucker lean rats were purchased from Japan SLC (Shizuoka, Japan). Diet-induced obese (DIO) mice were obtained by 10-week feeding of a high-fat diet (32% safflower oil, 33.1% casein, 17.6% sucrose, and 5.6% cellulose[13]) beginning at 5 weeks of age. β1/β2/β3 adrenergic receptor triple knockout (β-less) mice[18] were provided by Dr B. B. Lowell.

Administration of recombinant adenovirus

Recombinant adenoviruses bearing murine PPARγ2 cDNA,[13] the bacterial β-galactosidase gene,[13] DGAT1, DGAT2,[19] or fat-specific protein 27 (Fsp27)[20] cDNA, and for RNA interference, recombinant adenovirus encoding short-hairpin RNA for PPARγ, scramble (AdK7-H1-scramble),[13] or FSP27[20] were injected into mice (see Supplementary material online for details).

Blood analysis

Blood glucose was assayed with Antsense II (Horiba Industry, Kyoto, Japan). Serum insulin and leptin were determined with enzyme-linked immunosorbent assay kits (Morinaga Institute of Biological Science, Yokohama, Japan).

Blood pressure (BP) measurement

Systolic blood pressure (SBP) was usually determined by the standard tail-cuff noninvasive measurement system[21] using a model MK-2000 sphygmomanometer for mice and rats (Muromachi Kikai, Tokyo, Japan) according to the manufacturer's instructions. The tail-cuff system is commonly used for measuring SBPs in conscious animals without operative intra-arterial catheterization, and the results reportedly correspond to those obtained with telemetry.[22] At least six readings were obtained for each experiment, and a mean value was assigned to each individual mouse and rat.

Dissection of hepatic branch of the vagus

Selective hepatic vagotomy was performed as previously described[13] (see Supplementary material online for details).

Selective hepatic vagal afferent blockade by perivagal application of capsaicin

Selective blockade of hepatic vagal afferent was performed by perivagal application of capsaicin.[13] The hepatic branch of the vagal trunk was isolated from surrounding tissues using paraffin films, then loosely tied with a cotton string with or without being immersed in capsaicin (Sigma Chemical Co, St Louis, MO, USA) dissolved in olive oil (5% wt/vol) (see Supplementary material online for details).

Hepatic triglyceride content

Frozen livers were homogenized and triglycerides were extracted with $CHCl_3$:CH_3OH (2:1, v:v), dried and resuspended in 2-propanol.[13] Triglyceride contents were measured using Lipidos liquid (TOYOBO, Osaka, Japan).

Immunoblotting and histological analysis

Immunoblotting was performed as previously described[13] using anti-PPARγ antibody (Cell Signaling Technology, Danvers, MA, USA). Hepatic vagal nerve immunohistochemistry was performed as previously described[13] (see Supplementary material online for details).